Unconventional quantum criticality emerging as a new common language of transition-metal compounds, heavy-fermion systems, and organic conductors

2010 J. Phys.: Condens. Matter 22 164206

(http://iopscience.iop.org/0953-8984/22/16/164206)

IOP Publishing Journal of Physics: Condensed Matter

J. Phys.: Condens. Matter **22** (2010) 164206 (9pp) doi:10.1088/0953-8984/22/16/164206

Unconventional quantum criticality emerging as a new common language of transition-metal compounds, heavy-fermion systems, and organic conductors

Masatoshi Imada, Takahiro Misawa and Youhei Yamaji

Department of Applied Physics, University of Tokyo and JST-CREST, Hongo, Bunkyo-ku, Tokyo, Japan

E-mail: imada@ap.t.u-tokyo,ac,jp

Received 12 June 2009, in final form 24 January 2010
Published 30 March 2010
Online at stacks.iop.org/JPhysCM/22/164206

Abstract

We analyze and overview some of the different types of unconventional quantum criticalities by focusing on two origins. One origin of the unconventionality is the proximity to first-order transitions. The border between the first-order and continuous transitions is described by a quantum tricritical point (QTCP) for symmetry breaking transitions. One of the characteristic features of the quantum tricriticality is the concomitant divergence of an order parameter and uniform fluctuations, in contrast to the conventional quantum critical point (QCP). The interplay of these two fluctuations generates unconventionality. Several puzzling non-Fermi-liquid properties in experiments are taken to be accounted for by the resultant universality, as in the cases of $YbRh_2Si_2$, $CeRu_2Si_2$ and β-$YbAlB_4$. Another more dramatic unconventionality appears again at the border of the first-order and continuous transitions, but in this case for topological transitions such as metal–insulator and Lifshitz transitions. This border, the marginal quantum critical point (MQCP), belongs to an unprecedented universality class with diverging uniform fluctuations at zero temperature. The Ising universality at the critical end point of the first-order transition at nonzero temperatures transforms to the marginal quantum criticality when the critical temperature is suppressed to zero. The MQCP has a unique feature with a combined character of symmetry breaking and topological transitions. In the metal–insulator transitions, the theoretical results are supported by experimental indications for $V_{2-x}Cr_xO_3$ and an organic conductor κ-$(ET)_2Cu[N(CN)_2]Cl$. Identifying topological transitions also reveals how non-Fermi liquid appears as a phase in metals. The theory also accounts for the criticality of a metamagnetic transition in $ZrZn_2$, by interpreting it as an interplay of Lifshitz transition and correlation effects. We discuss the common underlying physics in these examples.

(Some figures in this article are in colour only in the electronic version)

1. Introduction

Quantum phase transitions and unconventional quantum phases are the subjects of recent intensive studies. In particular, a number of strongly correlated electron systems provide us with unconventional types of quantum critical behaviors frequently accompanied by wide areas exhibiting non-Fermi-liquid properties in metals. These range from rare-earth compounds [1–3], transition-metal compounds [4] and organic conductors [5], implying the existence of a universal underlying physics.

A prototype of quantum critical phenomena is found in the case where critical temperatures of spontaneous symmetry breaking, such as magnetic ordering, are suppressed to zero, as

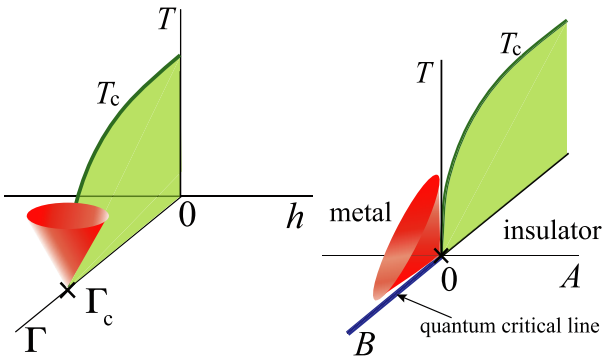

Figure 1. Phase diagram around conventional QCP (a) (left panel), and MQCP (b) (right panel for metal–insulator transition) in the parameter space of temperature T, fields to control transitions h or A and parameters to control quantum fluctuations Γ or B. The cone structures schematically illustrate the quantum critical regions of the QCP (a) and MQCP (b) depicted by the crosses. First-order transitions occur when one crosses shaded (green) walls. The quantum critical line (bold (blue) line) in (b) represents a continuous topological transition at $T = 0$.

we see in figure 1(a), by enhancing some quantum fluctuation Γ. The parameter Γ, enhancing the quantum fluctuations of magnetic, charge or orbital orders in electronic systems, is typically pressure or chemical doping, where itinerancy enhanced by these control parameters increases quantum fluctuations for the real space order realized by translational symmetry breaking. Enhancing geometrical frustration effects also increases quantum fluctuations. When the critical temperatures are suppressed to be low, low-energy and long-wavelength critical fluctuations of the order parameter start showing quantum mechanical character. In itinerant electron systems, this quantum critical fluctuation couples to low-energy quasiparticle excitations around the Fermi surface and leads to critical fluctuations qualitatively larger than the insulating case. This coupled case has been extensively studied by spin fluctuation theories developed by Moriya, Hertz and Millis [6–8]. A feedback of the critical fluctuations to the quasiparticle excitations leads to non-Fermi-liquid behaviors typically observed in the region of a cone-shape structure, as in figure 1(a). These standard spin fluctuation theories have been successful in explaining a number of experimental results on non-Fermi-liquid properties near the quantum phase transitions [6, 9].

However, this standard theory has widely been challenged by recent progress in experiments [1–3]. In some cases, critical exponents do not follow the prediction of the standard theory. In other cases, the critical region is unexpectedly large. An important aspect ignored in the standard theory of quantum criticality is the interplay of itinerancy with localization effects caused by electron correlations. Low-energy incoherent excitations on the verge of localization introduce a qualitatively new feature.

In addition, novel quantum criticality in nature emerges when quantum phase transitions are not the consequences of the symmetry breaking. A completely different type of unconventional quantum phase transitions appears associated with *topological change*, such as metal–insulator and Lifshitz transitions [10], when they are combined with electron correlation effects as we describe in this paper.

In this report, we first review the understanding recently achieved for several different types of unconventional quantum criticalities. Among various types of approaches for the unconventional quantum criticalities, we particularly focus on the cases where proximity to first-order transitions severely modifies the conventional quantum criticality. This universal aspect offers a key for solving many puzzles and for understanding unconventional features in experiments. The proximity to the first-order transitions is sometimes detected by signatures of spatial inhomogeneity and phase separations when the jump of the first-order transitions occurs in density under a fixed chemical potential. This inhomogeneity is the subject of recent intensive studies in systems with competing orders, although we do not go into the details of the issues of the inhomogeneity and phase separation.

A proximity to the first-order transitions in classical systems appears around the boundary between the continuous and first-order transitions called the tricritical point (TCP) [11], as is illustrated in figure 2(a). For example, at the TCP of an antiferromagnetic transition under magnetic fields [12], the jump of magnetization seen at the first-order transition is suppressed to zero, while a singular divergence of the magnetization slope as a function of magnetic fields appears. Then a unique feature of the TCP driven by magnetic fields is that the *uniform* magnetic susceptibility at zero wavenumber diverges, in addition to the diverging order parameter susceptibility at a nonzero wavenumber, although it does not have a tendency for the ferromagnetic order at all. If the critical temperature of the TCP is suppressed to zero, this transforms to a QTCP, as we illustrate in a schematic phase diagram figure 2(b). We discuss in section 2 how an unconventional criticality appears in the case of the QTCP of the antiferromagnetic transition under magnetic fields [13, 14], which has relevance in a number of f electron systems including $YbRh_2Si_2$, $CeRu_2Si_2$ and β-$YbAlB_4$. We also discuss possible origins of the proximity to first-order transitions, such as magnetic anisotropy and valence instability.

The proximity to the first-order transition appears in a more dramatic way in the case of the topological change. A simple example of the topological change is found in a Fermi surface change such as a Lifshitz transition and a metal–insulator transition between a band-insulator and a metal. Although these topological transitions offer continuous quantum phase transitions, they do not cause any spontaneous symmetry breaking by themselves, while the critical phenomena are rather trivial in noninteracting systems. However, electron correlation introduces unprecedented effects. When the correlation effects become large, these transitions may become first-order transitions. The first-order transition continues to finite temperatures and is terminated at the finite temperature critical point. Then this is well characterized by the conventional universality class of symmetry breaking, where a similarity to the gas–liquid transition may be identified. The boundary between the first-order and conventional continuous topological transitions illustrated in figure 1(b) contains both the characters of

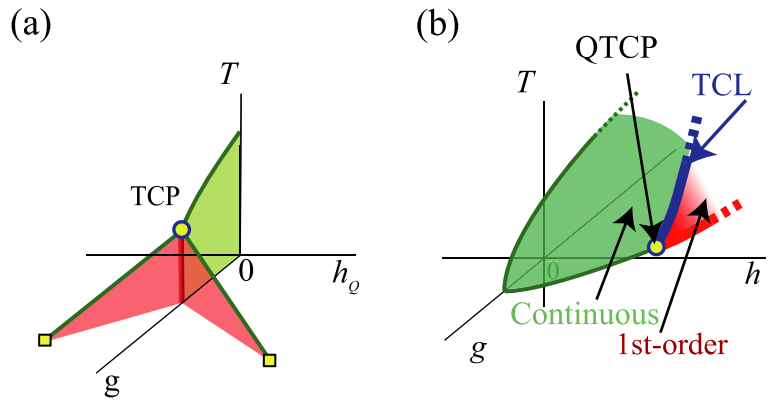

Figure 2. (a) Schematic phase diagram for continuous and first-order transitions together with classical TCP in the parameter space of temperature T, quantum fluctuation g and field h_Q conjugate to the order parameter m_Q. Thin (green) lines represent critical lines of continuous transitions, while the route crossing the shaded sheets realize first-order transitions. At $h_Q = 0$, the bold (red) line represents the first-order transition as well. The circle is the classical TCP while the squares illustrate the QCP. (b) Global phase diagram with a tricritical line (TCL) separating the surfaces of the continuous (above TCL (green)) and the first-order (below TCL (red)) surfaces. Here g represents a parameter to control quantum fluctuations. In $YbRh_2Si_2$, g may correspond to the pressure measured from the ambient one and h may be the uniform magnetic field. The QTCP (circle) appears at $(g, H, T) = (g_t, H_t, 0)$, namely the endpoint of the TCL at $T = 0$.

the topological and symmetry breaking transitions [15–18]. This point, called the MQCP, induces novel quantum critical phenomena around it. We clarify this novel physics in cases of metal–insulator transitions in section 3.1 and Lifshitz transitions in section 3.2.

The first-order transition and its proximity around the MQCP are the consequence of strong correlation effects, though the topological nature survives. This compatibility is more deeply understood by the differentiation of quasiparticles in the momentum space. The electron differentiation appears in such a way that some particular part in the Brillouin zone shows strong correlation effects with precursory insulating behavior while it leaves the other part coherent as a small pocket of the Fermi surface. The transition takes place as a topology change through the vanishing pockets [19, 20]. The topological nature is better understood from the role of the zeros of the Green function (the poles of the self-energy), where the emergent zeros nonuniformly destroy the large Fermi surface and leave the small pocket.

Through analyses on different types of the proximity to the first-order transition, in this paper, we discuss the underlying common physics with its relevance to experimental results for unconventional quantum critical phenomena.

2. Quantum tricriticality

In the classical Ginzburg–Landau–Wilson (GLW) scheme, the TCP is expressed by the ϕ^6 theory [11]. The free energy F is expanded up to the sixth order with respect to the scalar order parameter m_Q representing a spatial symmetry breaking at the wavenumber Q as

$$F = rm_Q^2 + um_Q^4 + vm_Q^6 - h_Q m_Q. \tag{1}$$

If $u > 0$, $r = 0$ together with vanishing fields conjugate to the order parameter, $h_Q = 0$ represent a conventional Ising-type critical point. If $u < 0$, $u^2 - 3rv > 0$ and $h_Q = 0$, three minima at $m_Q = 0$ and $\pm m_{Q0}$ with $m_{Q0} \equiv \sqrt{(-u + \sqrt{u^2 - 3rv})/3v}$ can represent the first-order transition between $m_Q = 0$ and $\pm m_{Q0}$. At $h_Q = 0$, the first-order transition for $u < 0$ and the continuous transition at $r = 0$ for $u > 0$ merge at $r = u = 0$, which determines the TCP. Physics of the TCP has extensively been discussed for the mixture of ^{3}He and ^{4}He as well as for antiferromagnetic transitions under magnetic fields [11]. A characteristic feature of the TCP is that not only the order parameter susceptibility diverges as $\chi_Q = (\partial^2 F/\partial m_Q^2)^{-1} = 1/r \propto 1/(h - h_c)$ in this mean-field theory, but also the uniform susceptibility $\chi_0 = (\partial^2 F/\partial h^2)$ diverges, when the transition is controlled by uniform fields h around the critical point $h = h_c$. In fact, m_Q is scaled by $m_Q \propto r^{1/4} \propto |h - h_c|^{1/4}$ at $u = 0$ and the resultant scaling of the free energy minimum $F \propto |h - h_c|^{3/2}$ leads to $\chi_0 \propto |h - h_c|^{-1/2}$. This indicates the scaling of the uniform magnetization $m_0 - m_{0c} \propto \sqrt{m_Q}$ when m_0 is measured from the critical value m_{0c}. We note that this diverging χ_0 as $h \to h_c$ has nothing to do with the ferromagnetic tendency but is just the consequence of the tricriticality of the antiferromagnetic transition. Because of the vanishing u and r, the free energy becomes flattened around $m_Q = 0$ and hence fluctuations around the critical point become large in general. It also causes the diverging uniform susceptibility.

When the tricritical temperature is suppressed by quantum fluctuations, the QTCP appears. In this case, when the transition occurs in metallic phases, the critical fluctuations of bosons associated with the order parameter fluctuations couple to the low-energy quasiparticle excitations near the Fermi surface similarly to the conventional QCP in metals [6, 8]. However, in the case of the QTCP, it has features qualitatively different from the conventional quantum criticality already known in the classical case. To elucidate this, we have proposed a spin fluctuation theory for the antiferromagnetic QTCP [13, 14]. As in the classical case, under magnetic fields, 'ferromagnetic' quantum critical fluctuations develop around the antiferromagnetic QTCP in addition to antiferromagnetic

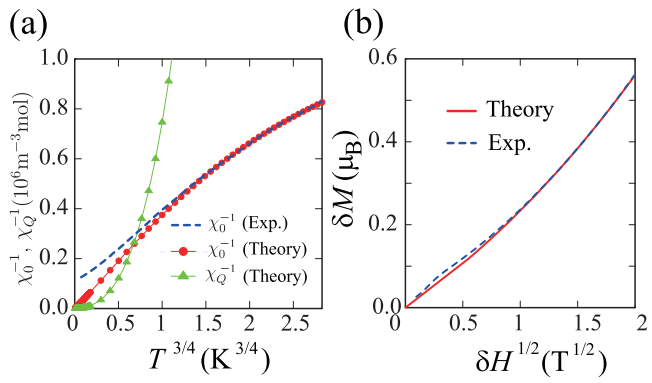

Figure 3. (a) Temperature dependence of inverse uniform magnetic susceptibility χ_0^{-1} for $YbRh_2(Si_{0.95}Ge_{0.05})_2$ at $H = 0.03$ T reported in [23] illustrated as the broken (blue) curve compared with the numerical result of spin fluctuation theory for the QTCP [13, 14], shown as the solid (red) curve with filled circles. The deviation at low temperatures appears because the experimental parameters deviate from the QTCP. The solid (green) curve with triangles represents the theoretical χ_Q^{-1}. (b) Magnetic field dependence of magnetization (broken (blue) curve) for $YbRh_2(Si_{0.95}Ge_{0.05})_2$ at $T = 0.09$ K reported in [23] compared with the QTCP theory (solid (red) curve) [13, 14]. δM (δH) represents the magnetization (magnetic field) measured from the critical value. We estimate the experimental critical magnetic field H_c (magnetization M_c) as 0.027 T (0.004 μ_B).

fluctuations, which is in sharp contrast with the conventional antiferromagnetic QCP. For itinerant electron systems, it has been shown that the temperature dependence of critical magnetic fluctuations around the QTCP is given as $\chi_Q \propto T^{-3/2}$ ($\chi_0 \propto \sqrt{\chi_Q} \propto T^{-3/4}$) at the antiferromagnetic (ferromagnetic) wavenumber $q = Q$ ($q = 0$). The convex temperature dependence of $\chi_0^{-1} \propto T^{3/4}$ is the characteristic feature of the QTCP, which should not be seen in the conventional spin fluctuation theory for the ferromagnetic transition because the exponent 3/4 is smaller than unity for the Curie law. The same scaling leads to the singular magnetization process $m \propto |h - h_c|^{1/2}$. It should be noted that these critical exponents are completely different from the conventional quantum criticality.

It has been shown that physics of the QTCP accounts for several unconventional features of the quantum criticalities and non-Fermi-liquid properties observed experimentally in heavy-fermion systems such as $YbRh_2Si_2$, $CeRu_2Si_2$, and β-$YbAlB_4$ [13, 14]. For $YbRh_2Si_2$, the QTCP successfully reproduces quantitative behaviors of the experimental ferromagnetic susceptibility $\chi_0 \propto T^{-0.6}$ by an appropriate choice of the phenomenological parameters. In fact, a crossover from $\chi_0 \propto T^{-3/4}$ to $\chi_0 \sim T^{-0.6}$ with elevated temperatures predicted by the theory of the QTCP quantitatively reproduces the experimental result, as seen in figure 3(a). The deviation at low temperatures is ascribed to the deviation of the experimental parameters from the right QTCP. Figure 3(b) also shows that the magnetization curve follows the prediction of the quantum tricriticality $m \propto |h - h_c|^{0.5}$.

The quantum tricriticality also reproduces singularities of other physical properties such as specific heat, nuclear magnetic relaxation time $1/T_1T$, and the Hall coefficient observed for $YbRh_2Si_2$. A simple argument [21] predicts that the Hall coefficient R_H is scaled by $R_H \propto m_Q^{\dagger\,2}$, while as is mentioned above, $m_Q \propto |h - h_c|^{1/4}$ holds. Therefore, the Hall coefficient is scaled by $|h - h_c|^{1/2}$ near the QTCP. This scaling indicates that the Hall coefficient shows a singular change near the QTCP. If the QCP in $YbRh_2Si_2$ is located on the side of weak first-order phase transitions, the Hall coefficient changes even jump at $T = 0$. A steep increase of R_H in the experiment [22] at low temperatures is consistent with the present prediction.

Under magnetic fields $h > h_c$, two characteristic temperature scales are suggested in $YbRh_2Si_2$ [23, 24]; below one scale (T_{LFL}), the Landau Fermi liquid becomes satisfactory while around the other scale T^*, $\partial R_H/\partial H$, $\partial\rho/\partial H$, and χ_0 have peaks. We note that the coexistence of the antiferromagnetic and ferromagnetic fluctuations is a possible origin of the observed two energy scales: T^* is interpreted as the energy scale where the uniform fluctuation χ_0 starts saturating and the response to the uniform magnetic field shows an anomaly. The other is T_{LFL}, below which the antiferromagnetic fluctuations saturate. Since the growth of the antiferromagnetic and uniform fluctuations both destroy the Fermi liquid scaling, the real Fermi liquid shows up only when both of them saturate, namely only below the lower scale T_{LFL}. Since both FM and AFM fluctuations diverge at the QTCP, two energy scales T^* and T_{LFL} vanish at the QTCP. This is consistent with the experimental result.

Recently, it has been pointed out that the specific heat exponent for the tricriticality scales as $C \propto |T - T_c|^{-1/2}$ [25, 14] This is consistent with the experimental observation [26].

The proposal for the proximity of the first-order transition and the tricriticality is also supported from the real existence of the first-order transition under pressure [27], where the jump of the resistivity is clearly seen at 2.3 GPa under the magnetic field $H \parallel c$ around 2 T. Since the tricritical temperature is around 0.5 K at this pressure, while the transition is always continuous at ambient pressure, the QTCP has to show up between these two pressures. The physics of QTCP can be more definitely tested at this anticipated QTCP and we propose experiments under the tuning of pressure. Recently, effects of chemical pressure have been examined by substituting Co for Rh [28]. It suggests a complex phase diagram: for a small concentration of Co up to $x = 0.28$ for $Yb(Rh_{1-x}Co_x)_2Si_2$, the transition becomes broadened without an indication of the first-order transition under magnetic fields perpendicular to the c axis. On the other hand, a first-order transition is signaled for large $x \sim 0.68$ under magnetic fields parallel to the c axis and even in the absence of magnetic fields. The absence of the first-order transition at small x was claimed [28] to contradict the experiment under hydrostatic pressure [27], if the chemical pressure and hydrostatic pressure could be mapped. However, since the first-order transition under hydrostatic pressure is observed only in magnetic fields parallel to the c axis, it is required to examine the chemical pressure effect under the same condition, because the mechanism may involve the effect of magnetic anisotropy, as we will discuss below.

For $CeRu_2Si_2$ [29] and β-$YbAlB_4$ [30] as well, the quantum tricriticality is a presumable origin of the anomalous

diverging enhancement of the uniform susceptibility observed in these materials [14].

Let us discuss mechanisms of generating first-order transitions. It is known that $YbRh_2Si_2$ and β-$YbAlB_4$ have a strong magnetic anisotropy. In fact, the QCP for $YbRh_2Si_2$ is realized at $\sim$0.06 T for the magnetic field perpendicular to the c axis while 0.6 T is required for the field parallel to the c axis. In classical metamagnetic systems, the single-site anisotropy commonly causes a first-order (metamagnetic) transition from an antiferromagnetic phase to a spin-flipped paramagnetic phase under magnetic fields, as in the case of $FeCl_2$ [31]. The first-order transition under pressure is so far observed only in magnetic fields parallel to the c axis [27], which may be related to this type of the mechanism.

Another possible origin driving the first-order transition is the valence instability in the f electron systems. The f electrons located near the Fermi level can hybridize with the conduction electrons c leading to the emergence of heavy-mass quasiparticles through the Kondo effect. The valence of the f electrons may abruptly change through the shift of the f electron level relative to the conduction electrons c and/or the competition among the conduction bandwidth, the c–f hybridization, and the atomic f–f as well as c–f electron correlations. This transition may lead to the formation/destruction of the f electron local moment. This dominates the physics of the γ–α transition of Ce [32]. The valence transition sometimes occurs as a first-order transition. If it happens as the first-order jump, the universality of the valence transition is described by the type of the gas–liquid transition with a finite temperature critical point characterized by the Ising universality. When this critical temperature is suppressed to zero, a conventional QCP that is equivalent to that in figure 1(a) appears.

Now, if the valence transition equivalently described by figure 1(a) occurs simultaneously with the magnetic transition, this valence critical point (T_c line in figure 1(a)) may be transformed to the tricritical point (tricritical line). This is because even outside the shaded (green) sheet in figure 1, the left and right sides of the shaded sheet have to be distinguished by the symmetry difference of the simultaneous magnetic transition. This means that the shaded (green) sheet continues to form a sheet of continuous transition beyond the T_c line. This is nothing but the appearance of the tricritical line that replaces the T_c line in figure 1. In this sense, the quantum tricriticality may capture relevant physics even when the valence transition is on the verge of the magnetic first-order transition.

A closely related idea is the localization transition of the f electron through the Kondo collapse (Kondo breakdown), namely the switch-off of the c–f hybridization disconnecting the f electrons from the conduction band, for example, through decreasing pressure. The Kondo collapse may take place either as a continuous or a first-order transition. When it is combined with a magnetic transition, the quantum tricriticality similar to the case of the valence transition may occur. Therefore, the quantum tricriticality may capture relevant physics even when the valence transition or the so-called local quantum criticality [21] is on the verge of the magnetic first-order transition.

On the other hand, if the valence transition or Kondo breakdown involves a topological change of the Fermi surface, the transition may have a structure essentially described by figure 1(b). In fact, this type of universality will be described in section 3. Here we note that the Kondo breakdown interpreted by the orbital-selective Mott transition of the f electrons indeed suggests the applicability of the universality discussed in section 3 [33, 34]. In this sense, the present classification and concept of unconventional quantum criticality offer a useful and general scheme for describing f electron systems.

3. Marginal quantum criticality

The proximity to the first-order transition appears in a different way when the underlying quantum criticality belongs to a different class. An intriguing issue is the quantum phase transition that is driven not by spontaneous symmetry breaking but by some topological change. In general, quantum phase transitions caused by a change in topological number occur in a wider class of phenomena, including the quantum Hall effects [35] and topological insulators [36]. A simple example is seen in the change in topology of the Fermi surface. In this section, we visit two examples of this category.

3.1. Metal–insulator transition

The first example is metal–insulator transitions driven by electron correlation effects. Such a well known example is the Mott transition [4].

In general, the metal–insulator transitions in weakly correlated systems take place either as the transition between Fermi liquids and band insulators or as the Anderson transitions driven by disorder. Both of these cases are essentially identified as the transitions at zero temperature. In these cases, unless some other origins such as a structural phase transition drive the metal–insulator transition and force discontinuous changes in the band structure through a strong electron–lattice coupling, the phase transitions are basically of continuous type.

However, when electron correlation effects play a role, transitions may frequently appear as first-order transitions. Even without a relevant coupling to the lattice, it is now believed that first-order transitions generically appear in nature. When the bandwidth is controlled either by pressure or chemical pressure realized through chemical substitutions, such first-order metal–insulator transitions are ubiquitously observed. A well known example is found for $V_{2-x}M_xO_3$ with M = Ti or Cr. In these compounds, the first-order transition terminates at around 350 K, identified as the critical point [37]. The universality class of this critical point has been studied carefully from the conductivity exponent and it has been established that it belongs to the Ising universality class [38]. Although the order parameter is not trivial, the transition is essentially described by the symmetry breaking type. It indicates that this Mott transition is equivalent to the gas–liquid transition that is known to be described by the Ising universality. In fact, the natural order parameter is the carrier density, as in the case of the density in the gas–liquid

transition. The Ising universality also implies that the transition is described by the conventional GLW scheme [39, 40]. This has immediately raised a fundamental question about the nature of this class of metal–insulator transition, because neither the metal to band-insulator transition nor the Anderson transition are known to belong to this universality class.

A successful phenomenological description is constructed starting from the free energy for the band-insulator metal transition. When the Fermi level crosses the bottom (top) of the band dispersion $\varepsilon(k) \propto k^z$ for electrons (holes), the free energy (or the energy at $T = 0$) of noninteracting electrons in the metallic phase is given by

$$F_0 \propto \int_0^{E_F} \mathrm{d}\varepsilon\, \varepsilon D(\varepsilon) \propto X^{(d+z)/d}, \tag{2}$$

where E_F is the Fermi energy and $D(\varepsilon) \propto \varepsilon^{(d-z)/z}$ is the density of states for spatial dimension d. The free carrier density is taken as the natural order parameter and defined as $X \geqslant 0$. In case of the generic dispersion expanded as $\varepsilon(k) \propto ak^2 + bk^4 + \cdots$, the free energy in the grand canonical ensemble is reduced to

$$F_0 \propto -\mu X + c_2 X^{(d+2)/d} + c_4 X^{(d+4)/d} + \cdots, \tag{3}$$

with constants c_2 and c_4 and the chemical potential μ for the carrier. In the insulating side, $F_0 = 0$ is trivially satisfied. Now the interaction energy may be introduced in the form of an effective two-body interaction of carriers scaled as

$$F_1 \propto X^2. \tag{4}$$

Then the total energy (free energy) in the metallic phase is given by

$$F = F_0 + F_1 = -\mu X + vX^2 + c_2 X^{(d+2)/d} + c_4 X^{(d+4)/d} + \cdots. \tag{5}$$

For $d = 1$, it turns out that the second lowest order term is proportional to c_2 while it is v for $d = 3$. Two-dimensional systems have a unique feature, because the terms proportional to c_2 and v are the same order. As we see below, this leads to an unconventional dynamical exponent $z = 4$ for the critical point $\mu = v + c_2 = 0$. It is now clear that though it has an expansion in terms of X, this form of the free energy does not follow the simple GLW scheme in any dimension. In fact when one moves the chemical potential as the control parameter, the expansion (5) is justified only in the metallic phase for larger μ, while the free energy in the insulator side described by smaller μ has the minimum zero always at $X = 0$, that means this piece-wise analytic character does not allow the analytic expansion of the free energy itself, in contrast to the case of equation (1). This breakdown originates from the fact that the metal–insulator transition between $X = 0$ and $X > 0$ is dominated by the topological character of the Fermi surface pocket on the verge of the transition. The transition is not originally described by any type of symmetry breaking but by the topological change in the ground state, where the singular form of the density of states D determines the nonanalytic expansion.

Let us focus on the two-dimensional case, where equation (5) is reduced to

$$F = AX + BX^2 + CX^3 + \cdots. \tag{6}$$

Then the effective interaction (quadratic term) is proportional to B. When B is positive, the metal–insulator transition occurs as a continuous transition by controlling A through zero. However, if the effective interaction B is driven to a negative value, a first-order transition occurs at a certain $A > 0$. The first-order transition is transformed to the continuous one at the MQCP determined by $B = 0$ and $A = 0$. The universality class of the MQCP is unconventional and is characterized by the critical exponents in the standard notation as

$$\begin{array}{llll} z = 4, & \alpha = -1, & \beta = 1, & \gamma = 1, \\ \delta = 2, & \nu = 1/2 & \text{and} & \eta = 0. \end{array} \tag{7}$$

For the parameter for the first-order transition, $B < 0$, the jump of X obviously continues to nonzero temperatures and the jump terminates at the critical point. For the critical point at $T > 0$, the free energy form (6) is no longer valid, because the singular form of D is immediately smeared out by the Fermi distribution at $T > 0$. Then the double minima form of the free energy expansion is regular as

$$F = -\mu X + A'X^2 + B'X^4 + \cdots, \tag{8}$$

which leads to the conventional Ising universality class [15–18]. Now it turns out that the MQCP is sandwiched by the topological quantum critical line for $B > 0$ at $T = 0$ and the Ising critical line at $T > 0$, as is sketched in figure 1(b). The unconventionality arises from this emergent character, which appears at the marginal point between the Ising-type symmetry breaking and the topological transition of the Fermi surface at zero temperature [15–18].

It has been shown that even Hartree–Fock approximations of an extended Hubbard model on square lattices are capable of such metal–insulator transitions with unusual criticality under a preexisting symmetry breaking [17, 18]. In this case, the above free energy expansion can indeed be obtained from microscopic models, analytically as well as numerically. The obtained universality perfectly agrees with the above critical exponents and with a number of numerical results beyond the mean-field level as well [41, 42], implying that the preexisting symmetry breaking assumed in the Hartree–Fock study is not necessary for this unconventional universality. Furthermore, examinations of fluctuation effects indicate that the critical exponents remain essentially exact beyond the mean-field level, except for the possible logarithmic correction, because the upper critical dimension d_c is given by [18]

$$d_c = \frac{\gamma + 2\beta}{\nu} - z = 2. \tag{9}$$

The critical exponents identified by the conductivity measurements for $V_{1-x}Cr_xO_3$ at finite temperatures [38] agree with the Ising exponents derived here. On the other hand, an organic conductor κ-$(ET)_2Cu[N(CN)_2]Cl$ has a low-temperature critical point of the metal-Mott-insulator

transition, where the same conductivity measurement has revealed unconventional exponents $\beta \sim 1, \gamma \sim 1$ and $\delta \sim 2$ [43]. These observations perfectly agree with the universality class of the MQCP.[1] In fact, the exponents for the MQCP at $T = 0$ survive as crossover exponents and dominate even at the nonzero-temperature critical point [18], as in the case of κ-$(ET)_2Cu[N(CN)_2]Cl$. The careful experimental results in $(V, Cr)_2O_3$ and κ-ET-type organic conductor κ-$(ET)_2Cu[N(CN)_2]Cl$ support the existence of the present marginal quantum criticality connecting the Ising-type critical line and the topological quantum critical line. The thermal expansion coefficient $\alpha(T) = l^{-1}\,\mathrm{d}l/\mathrm{d}T$ of κ-$(ET)_2Cu[N(CN)_2]Cl$ has also been reported to have an anomaly [46]. Since the data seem to strongly depend on the form of the distribution of the transition temperature, it is difficult to determine the exponent of the singularity quantitatively. Nevertheless, this anomaly can be qualitatively interpreted by the singularity of the mobile carrier density, because the lattice expansion linearly couples to the carrier density (see footnote 1). If the present quantum criticality also dominates for a uniform system, we expect the exponent of $\zeta = -1/2$ for $\alpha(T) \propto (T - T_c)^{\zeta}$, because the temperature axis crosses the transition from the metallic to insulator side and ζ generically probes $1/\delta - 1$.

To obtain direct evidence of the critical exponents, it is desirable to precisely determine the singularity of the carrier density. Finding a system with a lower critical temperature and revealing behaviors of Fermi surface topology are also very important challenges left for the future in this fundamental issue of the quantum Mott transition.

It is highly suggestive in terms of possible superconducting mechanisms that the MQCP emerges on the verge of the effective interaction of carriers driven to be attractive. Although the Ising critical point appears when the effective interaction is driven to be attractive, as in the case of the liquid–gas transition, for the superconducting pairing, the attractive interaction leading to the Cooper pairing has to be realized in the region of the Fermi degeneracy. This is only possible around the MQCP [44].

The present results imply that the metal–insulator transition is governed by a topological change in the Fermi surface with shrinkage (or emergence) at selected momentum points even when the interaction effects dominate. This is different from other types of scenario, such as that from the dynamical mean-field approximations, where the metal–insulator transition is governed instead by the vanishing renormalization factor Z and a large Fermi surface is retained even on the verge of the transition. On the verge on the metallic side, the topological character suggests that the Fermi surface is reduced to small pockets, which violates the Luttinger sum rule. If the system undergoes a Lifshitz transition from a large to a small Fermi surface, this violation is allowed on the side of the small pockets. The dynamical mean-field theory improved by including the momentum dependence of the self-energy indeed suggests the existence of such a Lifshitz transition [47], and the resultant shrinking small Fermi pockets in the absence of the translational symmetry breaking [20, 48].

In the mechanism of realizing the topological character of the metal–insulator transition, it has turned out that the zero of the single-particle Green function plays an important role [20, 49–51]. The single-particle Green function is defined as

$$G(k, \omega) = \frac{1}{\omega - \varepsilon(k) - \Sigma(k, \omega)}, \tag{10}$$

where Σ is the free energy and ε is the dispersion of the noninteracting part. Now, when ω is largely negative, $\mathrm{Re}\,G < 0$ must always be satisfied, while $\mathrm{Re}\,G > 0$ for largely positive ω. Thus a sign change has to occur at an intermediate value of ω at least once. In metals, the sign change indeed occurs through $\mathrm{Re}\,G = \pm\infty$, obtained from the pole of the Green function $\omega = \varepsilon(k) + \Sigma(k, \omega)$, which determines the Fermi surface of metals at $\omega = 0$. However, the sign change may also occur through $\mathrm{Re}\,G = 0$, which corresponds to the pole of the self-energy Σ. In fact, the above sign change in G has to occur between $\omega \gg 0$ and $\omega \ll 0$, even in insulators, while the Fermi surface does not exist in insulators at all. The sign change in insulators actually occurs through the zeros of the Green function. Since $\varepsilon(k) < 0$ at the Brillouin zone center (Γ point) while it is positive at the zone boundary (for example, at (π, π) in 2D systems), $\mathrm{Re}\,G$ has to change sign between these two point at $\omega = 0$, which determines the Fermi surface in metals. Even in the Mott insulator, this sign change equally has to occur; the only way in which this is possible is through the zeros of G. Therefore, a zero surface has to cross the Brillouin zone at $\omega = 0$.[2] Since the self-energy is divergent at the zeros, the perturbation expansion obviously breaks down at the zeros. For the continuous metal–insulator transitions, the poles cannot be replaced with the zeros abruptly at the transition, while poles completely disappear on the insulator side at $\omega = 0$ and the zeros dominate. This means that the emergence of the zeros has to already occur on the metallic side with a progressive replacement of the poles with zeros. When a topological transition ascribed to the interaction effects, such as a transition of zeros emergence or a Lifshitz transition, occurs at $\omega = 0$, this is the point of the breakdown of the Fermi liquid in the strict sense, and non-Fermi liquids show up, because the system is no longer adiabatically connected to the noninteracting system. It is clear that the breakdown of the Fermi liquid occurs in an inhomogeneous way in the Brillouin zone, depending on the distance from the zeros. Near the zeros, the quasiparticles become more incoherent because of the enhanced Σ and it introduces the differentiation of electrons. It has been shown that such a differentiation of electrons eventually leads to a breakup of the original large Fermi surface by the interference and penetration of the zeros to the poles. After the destruction of the original Fermi surface caused by the zeros, the remaining part of the Fermi surface becomes pockets and the pockets shrink to disappear at the *topological* metal–insulator transition. From this clarification, it turns out that the topological character of the metal–insulator transition clearly leads to the emergence of a non-Fermi liquid as an

[1] An attempt to justify both of these different criticalities within the scenario of the conventional Ising universality for the classical Mott transition has been given by [45].

[2] For an example of an insulator that does not require the zero surface at $\omega = 0$, contrary to the present discussions, see [52].

extended phase realized by the appearance of the zeros. Effects of zeros and differentiation of electrons on the thermodynamic as well as transport properties are not fully understood yet, and left as intriguing issues.

3.2. Lifshitz transition

A topological change in the Fermi surface called the Lifshitz transition was originally studied for noninteracting electrons [10]. Recently, interaction effects on the Lifshitz transitions have been systematically studied [53]. When the electron Coulomb interaction is switched on, a first-order transition may appear similarly to the case of the metal–insulator transition discussed in section 3.1. The marginal point between the continuous and first-order transition lines again appears as the MQCP. When the Lifshitz transition takes place in the ferromagnetic phase and the first-order transition is driven by magnetic fields, it also appears as a metamagnetic transition.

Similarly to the case of metal–insulator transitions described by equation (5), when a Fermi pocket vanishes at a Lifshitz transition, the free energy can be expanded by the magnetization Δm and magnetic field Δh, both measured from the critical point as [53]

$$F = -\Delta h \Delta m + v(\Delta m)^2 + c_2(\Delta m)^{(d+2)/2} + \cdots. \quad (11)$$

Equation (11) is obtained from $F_0 \propto (\Delta m)^{(d+z)/z}$ instead of equation (2), because of $\Delta m \propto E_F$ and $E_F \propto X^{z/d}$. If a neck of the Fermi surface changes its topology [53], it is expanded in two dimensions as

$$F = -\Delta h \Delta m + v(\Delta m)^2 + c_{2l}\frac{(\Delta m)^2}{\ln \frac{1}{|\Delta m|}} + c_4(\Delta m)^3 + \cdots, \quad (12)$$

and in three dimensions as inferred from equation (11) as

$$F = -\Delta h \Delta m + v(\Delta m)^2 + c_2(\Delta m)^{5/2} + c_3(\Delta m)^3 + \cdots, \quad (13)$$

for the disconnected side of the neck-collapsing transition and

$$F = -\Delta h(\Delta m) + v(\Delta m)^2 + c_3(\Delta m)^3 + \cdots, \quad (14)$$

for the connected side.

In fact, this mechanism in three-dimensional systems has been proposed to be relevant in the unconventional criticality of the metamagnetic quantum critical end point for $ZrZn_2$ [54]. Itinerant ferromagnets, such as $ZrZn_2$ [55, 56] and UGe_2 [57], and nearly ferromagnetic metals, such as $Sr_3Ru_2O_7$ [58], show metamagnetic transitions. The magnetizations show jumps at magnetic fields separating the low-field phase from the high-field phase with a higher magnetic moment. The first-order transition terminates at a finite temperature critical point. The universality around the critical point is again regarded as the Ising-type, which is equivalent to the gas–liquid critical points. The critical temperature can, however, be controlled to zero, for example, by pressure, which offers a QCP. A possible connection of these QCPs to non-Fermi-liquid behavior, as well as to the superconductivity found in UGe_2, has stimulated extensive studies [59].

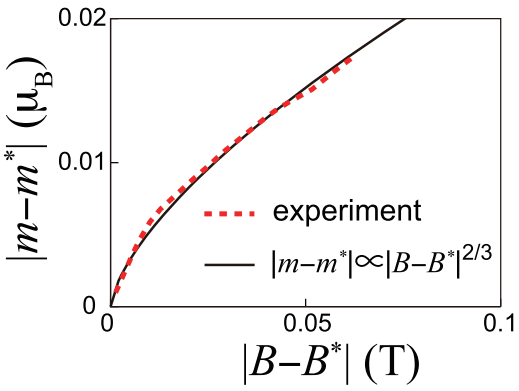

Figure 4. Magnetic field dependence of magnetization, both measured from the critical point. Theoretical prediction [54] of the MQCP plotted as the solid (black) curve reproduces the experimental results for $ZrZn_2$ given by the dashed (red) curve [56]. This is evidence for the MQCP described by $\delta = 3/2$.

These metamagnetic transitions have first been analyzed by the conventional framework of the quantum criticality of symmetry breaking [60]. However, it has been proposed that a topological change in the Fermi surface of the neck-collapsing type is responsible for the metamagnetic behavior for $ZrZn_2$, on the basis of the analyses by band structure calculation [54]. Then the free energy has the form of equations (13) and (14). In this case, the critical exponent δ, defined by $\Delta m \propto |\Delta h|^{1/\delta}$, is given by $\delta = 3/2$ for the side of the disconnected neck and $\delta = 2$ for the side of the connected neck. This is in sharp contrast with the Ising universality value $\delta \sim 4.8$. It is largely different even from the Ising mean-field value $\delta = 3$. This exponent predicts a convex curve for the inverse of uniform magnetic susceptibility χ_0^{-1} as a function of magnetization, as $\chi_0^{-1} \propto |\Delta m|^{1/2}$ on the disconnected side. This remarkable feature is consistent with the experimental indications by Uhlarz *et al* [56], as illustrated in figure 4.

4. Discussions

We have discussed mechanisms of several unconventional quantum criticalities associated with the proximity to first-order transitions. The first case is the quantum tricriticality in metals, where the conventional theory of quantum criticality for symmetry breaking transitions is substantially modified by the coupling of three low-energy modes, namely, uniform excitations, the order parameter, and quasiparticle excitations. The second case is topological transitions of a Fermi surface coupled to electron correlations, including metal–insulator transitions and Lifshitz transitions.

In all the cases, the proximity is a source of the unconventional non-Fermi liquid. The quantum tricriticality generates a crossover region of a non-Fermi liquid at nonzero temperatures while Fermi liquids are recovered at sufficiently low temperatures, except for the exact QTCP. On the other hand, if the symmetry breaking is suppressed, the continuous topological transitions accompany an extended area of a non-Fermi-liquid phase caused by the zeros of the Green function.

Although the MQCP generates a cone-shape structure of the critical region, similarly to the conventional quantum criticality, as we saw in figure 1(b), the unconventional metals have wider extension as a phase because of the electron differentiation caused by the penetrating zeros. In this respect, the physics of the metal–insulator and Lifshitz transitions awaits further studies, not only on the criticality, but also on the extended non-Fermi-liquid phase. First-order transitions may also introduce an extended spatially inhomogeneous region in the parameter space, including phase separations. Unexpectedly wide regions of non-Fermi liquids, recently pointed out in various experiments, may have a connection to this topological aspect combined with the proximity to the first-order transition[3]. Another intriguing issue is to elucidate the universality of the possible MQCP for other topological transitions, such as transitions of quantum Hall states and topological insulators.

Acknowledgments

The authors thank Yukitoshi Motome and Shiro Sakai for useful discussions and collaborations in part of this work. MI is also grateful to Phil W Anderson for fruitful discussions on [61]. This work has been supported by Grant-in-Aids from MEXT Japan.

References

[1] Stewart G R 2001 *Rev. Mod. Phys.* **73** 797
[2] Löhneysen H V, Rosch A, Vojta M and Wölfle P 2007 *Rev. Mod. Phys.* **79** 1015
[3] Gegenwart P, Si Q and Steglich F 2008 *Nat. Phys.* **4** 186
[4] Imada M, Fujimori A and Tokura Y 1998 *Rev. Mod. Phys.* **70** 1039
[5] Kanoda K 2006 *J. Phys. Soc. Japan* **75** 051007
[6] Moriya T 1985 *Spin Fluctuations in Itinerant Electron Magnetism* (Berlin: Springer)
[7] Hertz J A 1976 *Phys. Rev.* B **14** 1165
[8] Millis A J 1993 *Phys. Rev.* B **48** 7183
[9] Moriya T and Takimoto T 1995 *J. Phys. Soc. Japan* **64** 960
[10] Lifshitz I M 1960 *Sov. Phys.—JETP* **11** 1130
Lifshitz I M 1960 *J. Exp. Theor. Phys. (USSR)* **38** 1569
[11] For a review, see Lawrie I D and Sarbach S 1984 *Phase Transition and Critical Phenomena* vol 9, ed C Domb and J L Lebowitz (London: Academic) p 2
[12] Misawa T, Yamaji Y and Imada M 2006 *J. Phys. Soc. Japan* **75** 064705
[13] Misawa T, Yamaji Y and Imada M 2008 *J. Phys. Soc. Japan* **77** 093712
[14] Misawa T, Yamaji Y and Imada M 2009 *J. Phys. Soc. Japan* **78** 084707
[15] Imada M 2004 *J. Phys. Soc. Japan* **73** 1851
[16] Imada M 2005 *Phys. Rev.* B **72** 075113
[17] Misawa T, Yamaji Y and Imada M 2006 *J. Phys. Soc. Japan* **75** 083705
[18] Misawa T and Imada M 2007 *Phys. Rev.* B **75** 115121
[19] Tahara D and Imada M 2008 *J. Phys. Soc. Japan* **77** 093703
[20] Sakai S, Motome Y and Imada M 2009 *Phys. Rev. Lett.* **102** 056404
[21] Si Q, Rabello S, Ingersent K and Smith J L 2001 *Nature* **413** 804
Coleman P, Pépin C, Si Q and Ramazashvili R 2001 *J. Phys.: Condens. Matter* **13** R723
[22] Paschen S, Lühmann T, Wirth S, Gegenwart P, Trovarelli O, Geibel C, Steglich F, Coleman P and Si Q 2004 *Nature* **432** 881
[23] Gegenwart P, Custers J, Tokiwa Y, Geibel C and Steglich F 2005 *Phys. Rev. Lett.* **94** 076402
[24] Gegenwart P, Westerkamp T, Krellner C, Tokiwa Y, Paschen S, Geibel C, Steglich F, Abrahams E and Si Q 2007 *Science* **315** 969
[25] Shaginyan V R, Amusia M Ya and Popov K G 2009 arXiv:0905-1871v1
[26] Krellner C, Hartmann S, Pikul A, Oeschler N, Donath J C, Geibel C, Steglich F and Wosnitza J 2009 *Phys. Rev. Lett.* **102** 196402
[27] Knebel G *et al* 2006 *J. Phys. Soc. Japan* **75** 114709
[28] Klingner C, Krellner C and Geibel C 2009 arXiv:0908.1299v1
Krellner C, Klingner C, Geibel C and Steglich F 2009 arXiv:0910.3567v1
[29] Takahashi D, Abe S, Mizuno H, Tayurskii D A, Matsumoto K, Suzuki H and Onuki Y 2003 *Phys. Rev.* B **67** 180407(R)
[30] Nakatsuji S *et al* 2008 *Nat. Phys.* **4** 603
[31] Birgeneau R J, Shirane G, Blume M and Koeler W C 1974 *Phys. Rev. Lett.* **33** 1100
[32] Koskenmaki D C and Gschneidner K A 1978 *Handbook on the Physics and Chemistry of Rare Earths* vol 1, ed K A Gschneidner and L Eyring (Amsterdam: North-Holland) chapter 4
[33] Pepin C 2007 *Phys. Rev. Lett.* **98** 206401
[34] De Leo L, Civelli M and Kotliar G 2009 *Phys. Rev. Lett.* **101** 256404
[35] Thouless D J, Kohmoto M, Nightingale M P and den Nijs M 1982 *Phys. Rev. Lett.* **49** 405
[36] Kane C L and Mele E J 2005 *Phys. Rev. Lett.* **95** 146802
[37] McWhan D B, Pemeika J P, Rice T M, Brinkman W F, Maita J P and Menth A 1971 *Phys. Rev. Lett.* **27** 941
[38] Limelette P, Georges A, Jerome D, Wzietek P, Metcalf P and Honig J M 2003 *Science* **302** 89
[39] Landau L D, Lifshitz E M and Pitaevskii E M 1999 *Statistical Physics* (New York: Heinemmann)
[40] Wilson K G 1983 *Rev. Mod. Phys.* **55** 583
[41] Furukawa N and Imada M 1992 *J. Phys. Soc. Japan* **61** 3331
[42] Assaad F F and Imada M 1996 *Phys. Rev. Lett.* **76** 3176
[43] Kagawa F, Miyagawa K and Kanoda K 2005 *Nature* **436** 534
[44] Imada M 2005 *J. Phys. Soc. Japan* **74** 859
[45] Papanikolaou F *et al* 2008 *Phys. Rev. Lett.* **100** 026408
[46] de Souza M *et al* 2007 *Phys. Rev. Lett.* **99** 037003
[47] Hanasaki K and Imada M 2006 *J. Phys. Soc. Japan* **75** 084702
[48] Zhang Y Z and Imada M 2007 *Phys. Rev.* B **75** 045108
[49] Dzyaloshinskii I 2003 *Phys. Rev.* B **68** 085113
[50] Konik R M, Rice T M and Tsvelik A M 2006 *Phys. Rev. Lett.* **96** 086407
Yang K-Y, Rice T M and Zhang F-C 2006 *Phys. Rev.* B **73** 174501
[51] Stanescu T D and Kotliar G 2006 *Phys. Rev.* B **74** 125110
[52] Rosch A 2007 *Eur. Phys. J.* B **59** 495
[53] Yamaji Y, Misawa T and Imada M 2006 *J. Phys. Soc. Japan* **75** 094719
[54] Yamaji Y, Misawa T and Imada M 2007 *J. Phys. Soc. Japan* **76** 063702
[55] Kimura N 2004 *Phys. Rev. Lett.* **92** 197002
[56] Uhlarz M, Pfleiderer C and Hayden S M 2004 *Phys. Rev. Lett.* **93** 256404
[57] Huxley A, Sheikin I and Braithwaite D 2000 *Physica* B **284–288** 1277
[58] Perry R S *et al* 2001 *Phys. Rev. Lett.* **86** 2661
[59] Saxena S S *et al* 2000 *Nature* **406** 587
[60] Millis A J, Schofield A J, Lonzarich G G and Grigera S A 2002 *Phys. Rev. Lett.* **88** 217204
[61] Jain J K and Anderson P W 2009 *Proc. Natl Acad. Sci. USA* **106** 9131

[3] For the possibility of a more extended non-Fermi liquid phase, see [61].